Supporting Information for "Very low frequency earthquakes in between the seismogenic zone and the tremor zone in Cascadia?"

Wenyuan Fan[1], Andrew J. Barbour[2], Jeffrey J. McGuire[2], Yihe Huang[3], Guoqing Lin[4], Elizabeth S. Cochran[5], & Ryo Okuwaki[6]

[1]Scripps Institution of Oceanography, UC San Diego, La Jolla, California, USA
[2]U.S. Geological Survey, Earthquake Science Center, Moffett Field, California, USA
[3]Department of Earth and Environmental Sciences, University of Michigan, Ann Arbor, Michigan, USA
[4]Rosenstiel School of Marine and Atmospheric Science, University of Miami, Miami, Florida, USA
[5]U.S. Geological Survey, Earthquake Science Center, Pasadena, California, USA
[6]Mountain Science Center, Faculty of Life and Environmental Sciences, University of Tsukuba, Tsukuba, Ibaraki, Japan

Contents

Corresponding author: Wenyuan Fan, wenyuanfan@ucsd.edu

Dynamic and static strains

Table S1 lists the stations used in static strain analyses, and Table S2 lists the observed instrumental static strains (g) associated with VLFE event E3; these were determined by applying the Segmented Neighbor approach of *Barbour et al.* [2015] to lowpass filtered records. As described in the main text, the conversion from instrumental strains (g) to tensor strains (E) depends on a matrix of calibration coefficients C: $E = Cg$. Table S3 lists the calibration coefficients we used, which are from the tidal analyses of *Roeloffs* [2010] and *Hodgkinson et al.* [2013].

Table S1. Stations used in static strain analyses

Station	Longitude	Latitude	Distance to E3 [km]
B003	-124.1409	48.06236	34.0
B004	-124.4270	48.20192	47.5
B014	-123.8125	47.51330	48.4
B007	-123.5041	48.05757	68.4
B001	-123.1314	48.04307	93.5
B013	-122.9108	47.81300	105.6
B009	-123.4512	48.64867	116.1
B010	-123.4513	48.65017	116.2
B011	-123.4482	48.64954	116.3
B926	-124.1312	48.82020	116.4

Table S2. Static offsets at each station from VLFE event E3 (g matrices)

Station	CH0	CH1	CH2	CH3
B003	-1.5	-0.26	-0.74	-0.46
B004	-2.6	-0.52	0.9	0.14
B014	5.6	8.0	3.1	2.0
B007	-2.6	-9.7	5.5	-1.6
B001	1.8	2.0	-2.8	-1.6
B013	0.86	-0.23	0.97	-0.62
B009	-1.9	-0.097	-0.27	-1.0
B010	-0.34	-0.89	-1.2	-1.2
B011	-1.2	-0.88	1.6	-1.2
B926	0.9	0.3	0.52	0.39

Table S3. Calibration coefficients for C matrices

Station	Component	CH0	CH1	CH2	CH3
B003	Eee+Enn	0.2960	0.5180	0.2960	0.2220
B003	Eee-Enn	0.2090	-0.3450	-0.0715	0.2070
B003	2·Een	0.3310	0.1350	-0.3850	-0.0811
B004	Eee+Enn	0.2970	0.5180	0.2960	0.2220
B004	Eee-Enn	-0.2890	0.2980	0.1690	-0.1780
B004	2·Een	-0.2660	-0.2200	0.3530	0.1320
B014	Eee+Enn	0.2960	0.5190	0.2960	0.2220
B014	Eee-Enn	0.2700	-0.3120	-0.1450	0.1870
B014	2·Een	0.2840	0.2000	-0.3640	-0.1200
B007	Eee+Enn	0.2960	0.5180	0.2960	0.2220
B007	Eee-Enn	-0.3890	0.0258	0.3790	-0.0155
B007	2·Een	0.0470	-0.3700	0.1010	0.2220
B001	Eee+Enn	0.2960	0.5180	0.2960	0.2220
B001	Eee-Enn	-0.3650	-0.0669	0.3920	0.0401
B001	2·Een	0.1420	-0.3640	0.0034	0.2190
B013	Eee+Enn	0.2960	0.5190	0.2960	0.2220
B013	Eee-Enn	-0.0390	-0.3550	0.1810	0.2130
B013	2·Een	0.3900	-0.1060	-0.3480	0.0635
B009	Eee+Enn	0.0000	0.6670	0.0000	0.6670
B009	Eee-Enn	0.6850	-0.3240	0.0000	-0.3610
B009	2·Een	0.3520	0.2090	0.0000	-0.5600
B010	Eee+Enn	0.0000	0.6670	0.0000	0.6670
B010	Eee-Enn	0.6350	-0.3470	0.0000	-0.2880
B010	2·Een	0.4350	0.1660	0.0000	-0.6010
B011	Eee+Enn	1.3300	0.0000	1.3300	-1.3300
B011	Eee-Enn	0.0000	0.0000	0.6670	-0.6670
B011	2·Een	-0.7700	0.0000	-0.3850	1.1500
B926	Eee+Enn	0.0000	0.6670	0.0000	0.6670
B926	Eee-Enn	-0.0965	-0.3070	0.0000	0.4030
B926	2·Een	0.7640	-0.2330	0.0000	-0.5310

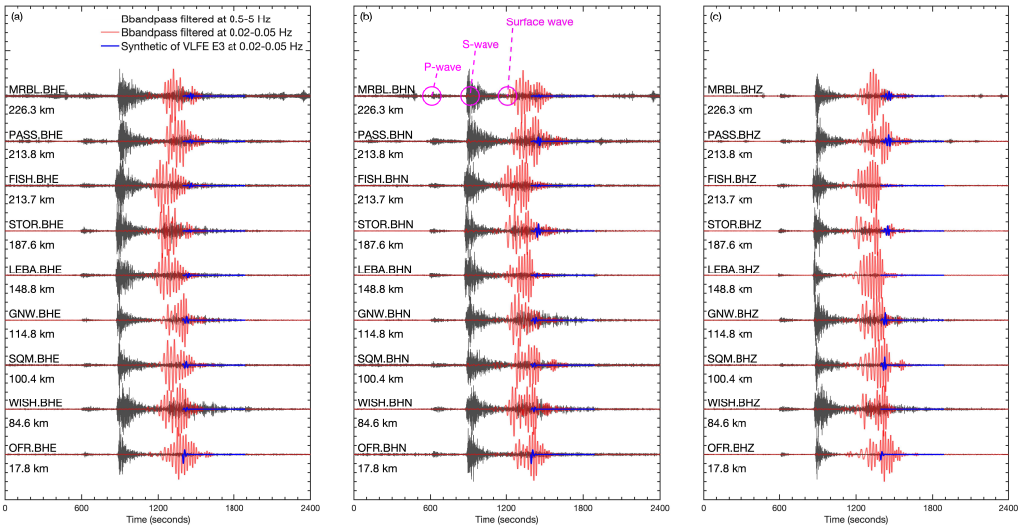

Figure S1. Near-field seismic records in the Pacific Northwest. Station distribution is listed in Figure 1, inset. The station name, component, and distance to E3 are listed by the trace. Time 0 s starts from 2009/08/03, 17:50:00. (a), self-normalized broadband records of E component. (b), self-normalized broadband records of N component. (c), self-normalized broadband records of Z component. The high-frequency records (0.5–5 Hz) show clear body-wave phases (P- and S-waves) of the 2009 M6.9 Canal de Ballenas earthquake. The low-frequency records (0.02–0.05 Hz) show clear surface waves of the 2009 M6.9 Canal de Ballenas earthquake. No clear high-frequency seismic radiation of the VLFE E3 can be identified from the records. We use the preferred source model of VLFE E3 to compute synthetic seismograms at these stations, most of the associated surface waves are buried in the mainshock surface waves.

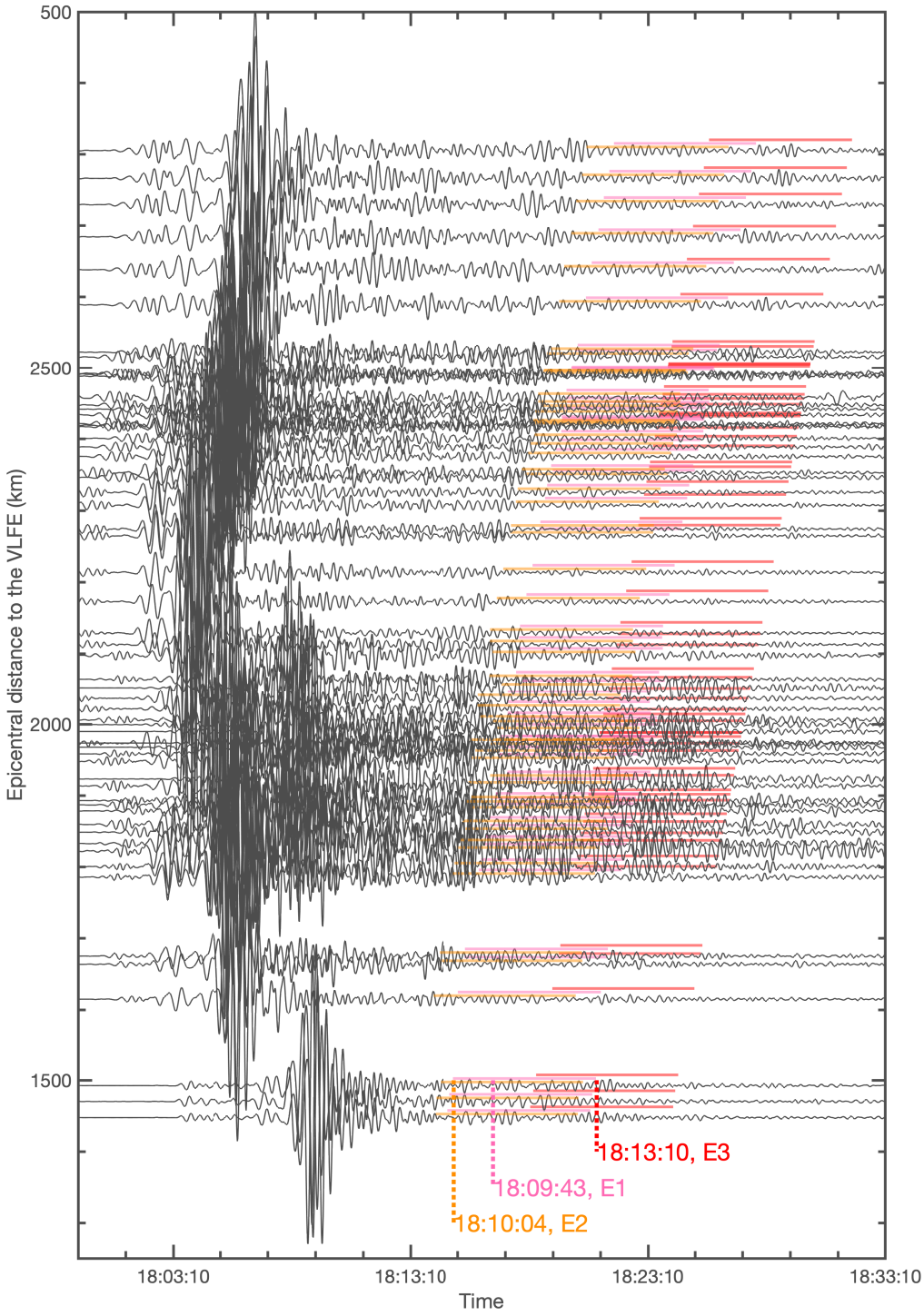

Figure S2. Record sections that are aligned with the epicenter of the VLFE E3 in Figure 2d. The records are self-normalized and bandpass-filtered to show signals in the 20–50 s period band. The pink, orange, and red bars indicate detection time windows for E1, E2, and E3, respectively. The E1 and E2 waveforms are less obvious comparing to those of E3.

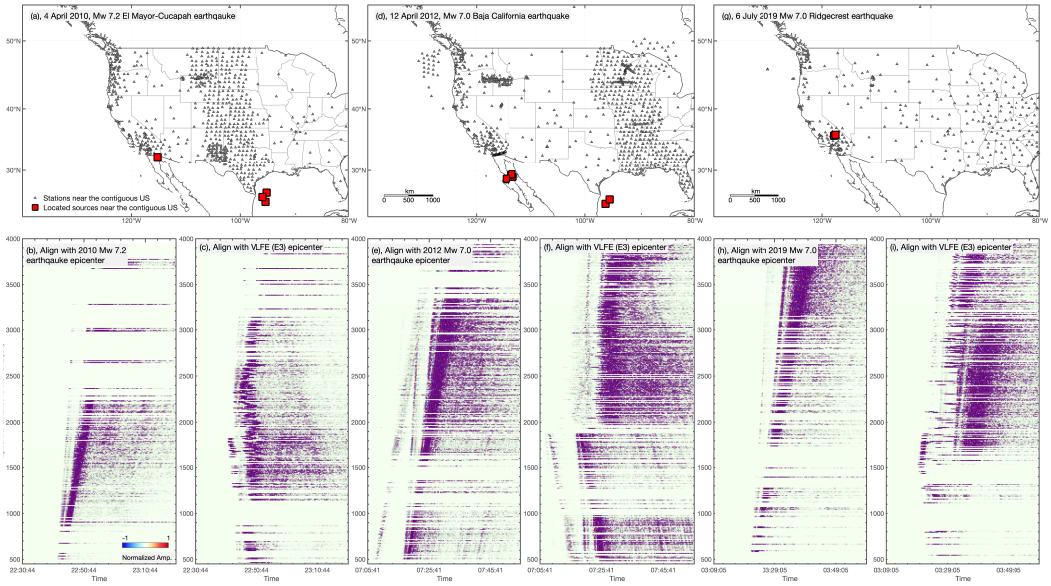

Figure S3. Detected seismic sources on 4 April 2010 (a), 12 April 2012 (d), and 6 July 2019 (g) and seismic records of the 2010 Mw 7.2 El Mayor-Cucapah earthquake (b–c), the 2012 Mw 7.0 Baja California earthquake (e–f), and the 2019 Mw 7.0 Ridgecrest earthquake (h–i). The record sections are one-hour record sections that are aligned with the earthquake epicenters (b, e, h) and the epicenter of the VLFE E3 (c, f, i). The legends are similar to those of Figure 3. Both the 2010 Mw 7.2 El Mayor-Cucapah earthquake and the 2012 Mw 7.0 Baja California earthquake triggered submarine landslides (a, d) in the Gulf of Mexico [*Fan et al.*, 2020].

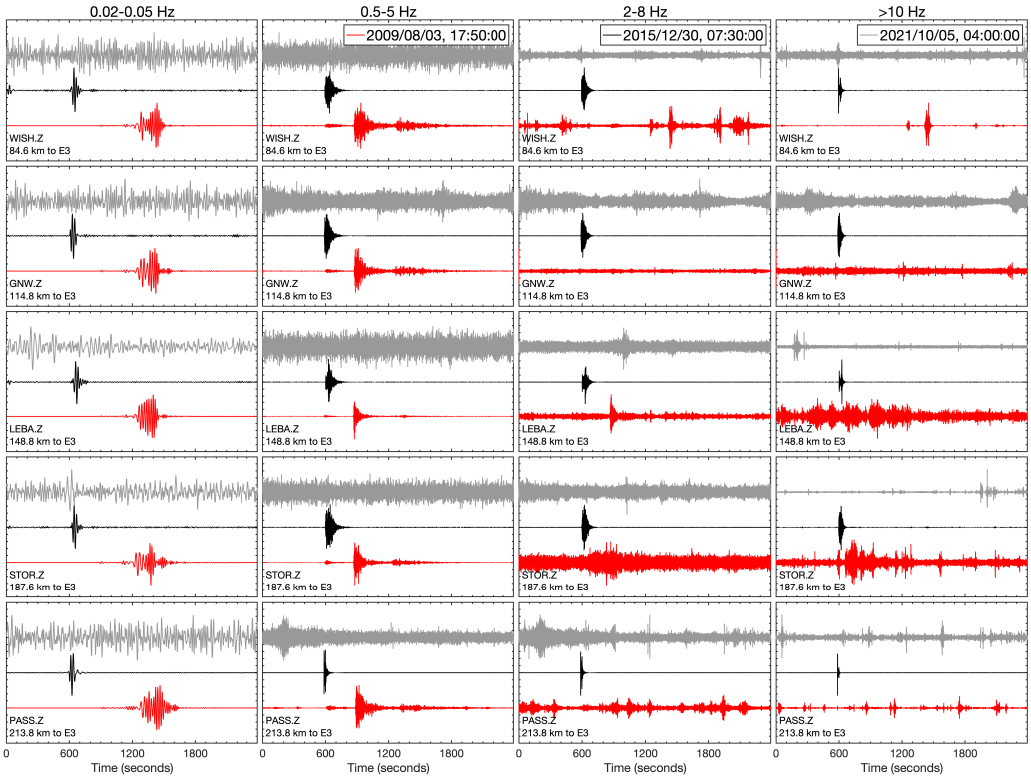

Figure S4. Near-field seismic records in the Pacific Northwest. Station distribution is listed in Figure 1, inset. The four columns show records filtered at four different frequency bands, including 0.02–0.05 Hz, 0.5–5 Hz, 2–8 Hz, and above 10 Hz. The five rows show records at five different stations with the station names listed at the lower left corners. The red traces show seismic records after the2009 M6.9 Canal de Ballenas earthquake as shown in Figure S1. The black traces show seismic records after a local M 4.8 normal faulting crustal earthquake (2015-12-30 07:39:29.310 UTC) that occurred near the southern most Vancouver Island. The gray traces show tremor records of the 2021 October episode that occurred near the M 4.8 earthquake. The comparison show that E3 is unlikely a local earthquake.

Open Research

The seismic data shown here were obtained from the Data Management Center (DMC) of the Incorporated Research Institutions for Seismology (IRIS). The strain data used to estimate offsets (Table S2) are from the Network of the Americas (NOTA) network and were also obtained from the IRIS DMC; this material is based on services provided by the Geodesy Advancing Geosciences and EarthScope (GAGE) facility, operated by UNAVCO.

References

Barbour, A. J., D. C. Agnew, and F. K. Wyatt (2015), Coseismic strains on Plate Boundary Observatory borehole strainmeters in Southern California, *Bulletin of the Seismological Society of America*, *105*(1), 431–444, doi:10.1785/0120140199.

Fan, W., J. J. McGuire, and P. M. Shearer (2020), Abundant spontaneous and dynamically triggered submarine landslides in the Gulf of Mexico, *Geophysical Research Letters*, *47*(12), e2020GL087,213.

Hodgkinson, K., J. Langbein, B. Henderson, D. Mencin, and A. Borsa (2013), Tidal calibration of Plate Boundary Observatory borehole strainmeters, *Journal of Geophysical Research: Solid Earth*, *118*(1), 447–458, doi:10.1029/2012jb009651.

Roeloffs, E. (2010), Tidal calibration of Plate Boundary Observatory borehole strainmeters: Roles of vertical and shear coupling, *Journal of Geophysical Research: Solid Earth*, *115*(B6), doi:10.1029/2009JB006407.